Research Article

Journal of Environmental Nanotechnology

Sustainable Fabrication of Nanoparticles from *Moringa Oleifera* Leaves and Their Efficiency During Photocatalytic Degradation of Mo and Mg Dyes

D.Ganesan[1*], Vigneshkumar Alagarsamy[2], S. Balasubramanian[3], S. Saileysh Sivaraja[4], Mohamed Khalif[5], S. Lokesh[6] and M. Durga[7]

[1]Department of Civil Engineering, Mahath Amma Institute of Engineering and Technology, Pudukkottai, TN, India
[2]Department of Civil Engineering, Mother Teresa College of Engineering and Technology, Pudukkottai, TN, India
[3]Department of Civil Engineering, Syed Ammal Engineering College, Ramanathapuram, TN, India
[4]Department of Civil Engineering, Saveetha Engineering College, Chennai, TN, India
[5]Department of Civil Engineering, C Abdul Hakeem College of Engineering and Technology, Melvisharam, TN, India
[6]Department of Civil Engineering, P.S.V College of Engineering and Technology, Krishnagiri, TN, India
[7]Department of Civil Engineering, Malla Reddy Deemed to be University, Hyderabad, TG, India
Received: 14.07.2026 Accepted: 10.08.2026 Published: xx.xx.xxxx
*ganesancivil.d@gmail.com

ABSTRACT

The ZnO nanoparticles (ZnO NPs) have good photocatalytic activity, but the traditional methods require the use of harmful chemicals, necessitating green methods for the synthesis of ZnO NPs. Now, in light of this research gap, the present study aims to synthesize ZnO NPs using *Moringa Oleifera* leaf extract and investigate the structural characteristics of the synthesized ZnO NPs, as well as their photocatalytic activity in the degradation of synthetic dyes. ZnO NPs were synthesized using the plant extract as a reducing agent and to stabilize the nanoparticles. The prepared ZnO NPs were characterized by UV-Vis, XRD, and EDX techniques in order to investigate the optical characteristics, crystallinity, and elemental surface composition of the prepared ZnO NPs, respectively. The photocatalytic activity of the prepared ZnO NPs was tested by the degradation of two textile dyes, namely MO and MG, under visible light illumination with different concentrations of the catalyst (10, 20, and 30 mg). The kinetic study of the photocatalytic activity of the prepared ZnO NPs was also assessed using zero-order, first-order, and second-order reaction models. The XRD result confirmed the formation of highly crystalline hexagonal ZnO NPs without any impurities (JCPDS 36-1451). The photocatalytic activity of the prepared ZnO NPs showed good activity in the degradation of the two textile dyes, with 76% of MO and 91% of MG being degraded by the ZnO NPs with a 30 mg dosage. *Moringa Oleifera* enables eco-friendly, low-cost, phytochemical-mediated ZnO nanoparticle synthesis efficiently.

Keywords: ZnO nanoparticles; Green synthesis; Photocatalytic degradation; Textile dyes; *Moringa Oleifera*; Wastewater treatment.

1. INTRODUCTION

Aquatic resources are unique among these key valuable resources on Earth, and life cannot endure without them. Every living organism, from microscopic bacteria to large animals, depends on clean water for survival and healthy growth (Zhao *et al.* 2026; Lee *et al.* 2026). However, rapid industrial development has brought serious environmental challenges, particularly the pollution of water bodies (Tella *et al.* 2025). Among these pollutants, synthetic dyes released from production, including fabrics, leather, plastics, and medications, pose one of the most severe threats. Large quantities of dyes are used daily, and a significant portion of them is discharged into natural water sources without proper treatment (Shinde *et al.* 2025; Periyasamy, 2025).

These dyes not only look bad but are also chemically stable, making them hard to break down (Kumar *et al.* 2025). The dyes' presence in water hampers the penetration of sunlight, affects the ecosystem, and can cause harmful health hazards for humans, such as toxicity, skin irritations, and long-term diseases (Farrag *et al.* 2025). However, the conventional treatment of wastewater does not effectively eliminate the dyes. The process can be expensive, require much energy, or use urban equipment, but the dyes will not be removed effectively (de Souza *et al.* 2025).

Nanotechnology emerges as a potent solution for the effective management of such persistent pollutants (Kristani *et al.* 2025). Amongst a number of nanostructures, ZnO NPs demand great attention owing to their superior photocatalytic properties that allow for the degradation of complex dye molecules under light exposure (Gul *et al.* 2025; Nguyen *et al.* 2025).

However, most of the conventional methods for the synthesis of ZnO nanoparticles have been found to be risky and expensive, involving harmful chemicals and instruments (El-Sheekh *et al.* 2025).

The green synthesis suggests a cleaner and more sustainable alternative, and instead of chemical agents, plants and other biological materials can act as natural "factories" for nanoparticle production. The plant extracts include an abundant mixture of secondary metabolites that naturally reduce and stabilize nanostructures, making this separation method simple, innocuous, and cost-effective (El-Khawaga *et al.* 2025; Mahajan *et al.* 2025).

The *Moringa Oleifera*, being readily available as a medicinal plant in India, can be considered the most suitable for the synthesis of nanoparticles through the green method due to the flavonoids, phenolic, tannic, alkaloid, and protein content present in the leaves (Singh *et al.* 2025; Rotimi *et al.* 2025). Plant-based ZnO nanoparticles have been studied in earlier research, but limited research has been done on the use of the *Moringa Oleifera* plant for the synthesis of ZnO nanoparticles and testing them for different dyes under different conditions (Sarwar *et al.* 2025; Aghajanyan *et al.* 2025; Thakur *et al.* 2025).

To identify the research gap, the present study emphasizes synthesizing ZnO NPs from Moringa Oleifera leaf mine, then examining their ability to degrade two commonly used dyes, MO and MG. Additionally, the study investigates the influence of pH, catalyst dosage, stability, and reusability on the light-activated catalytic productivity of these fabricated nanostructures. This research emphasizes the possibility of plant-extract nanotechnology, for example, a sustainable approach to water purification. By utilizing a readily available medicinal plant for nanoparticle synthesis, the study provides an environmentally safe, low-cost method that avoids toxic chemicals and complex procedures. The promising photocatalytic performance of the green-synthesized ZnO nanoparticles demonstrates their suitability for wastewater treatment, particularly in regions with limited resources. Figure 1 presents the process of green-synthesizing ZnO nanoparticles from *Moringa Oleifera* and their use in degrading synthetic dyes. The green synthesis of ZnO nanoparticles using *Moringa Oleifera* leaf extract resulted in the successful formation of ZnO nanoparticles with desirable structural, morphological, and optical properties. The synthesized nanoparticles exhibited excellent photocatalytic activity, achieving high degradation efficiencies for Methyl Orange (MO) and Malachite Green (MG). The study also demonstrated that the nanoparticles possess good stability and reusability, indicating their potential as an environmentally friendly and cost-effective photocatalyst for wastewater treatment.

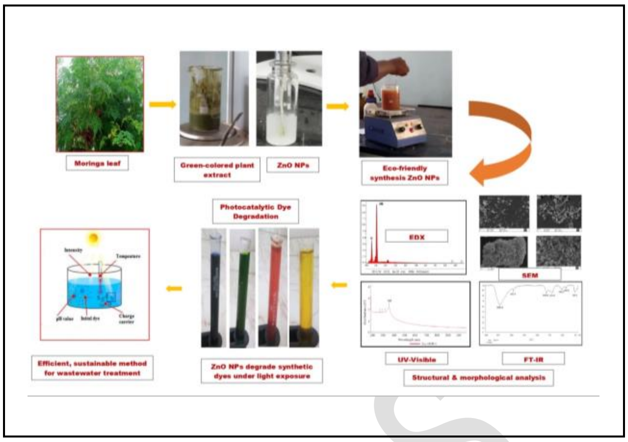

Fig. 1: Sustainable fabrication of ZnO NPs by *Moringa Oleifera* for dye treatment

2. MATERIALS AND METHODS

Zinc oxide and double-distilled water were obtained from MMC Laboratory Chemicals Pvt. Ltd., Chennai, India. The organic dyes, Methylene Orange (MO) and Malachite Green (MG), were purchased from Sigma-Aldrich.

2.1 Development from *Moringa Oleifera* Foliage Derivative

New *Moringa Oleifera* foliage was collected from local areas of Pudukkottai, Tamil Nadu. The foliage was carefully rinsed under flowing tap water to eliminate dirt and other contaminants, and then air-dried in the shade to preserve its expected phytochemicals. After being completely desiccated, the foliage was crushed and dried to a satisfactory consistency. Approximately 10 g of the crushed foliage was extracted using 250 mL of concentrated liquid in a Soxhlet apparatus at 60°C for about 10 minutes, or until the extract became pale in colour. Subsequently, to prevent chamber contamination, this extract was clarified through a Whatman No.1 filter paper. This filtrate was then centrifuged at 10,000 rpm for about 5 minutes towards obtain a clear supernatant, which served as the green precursor for ZnO nanoparticle fabrication. The analytical-grade zinc oxide (Sigma-Aldrich, Product No. 220299) was used for the preparation. A stock solution was prepared by dissolving 0.03 g of ZnO in 100 mL of concentrated liquid. This Moringa oleifera leaf extract was then mixed with the 1 mM ZnO solution in separate batches to facilitate the green fabrication of ZnO nanostructures (Sarwar *et al.* 2025; Nair *et al.* 2025; Olajide *et al.* 2025; Muthusamy *et al.* 2025; Abdelhameed *et al.* 2025).

2.2 Green Fabrication from ZnO NPs

The ZnO nanostructures were produced using a simple wet-chemical method. First, 100ml of the prepared *Moringa Oleifera* leaf extract was placed in a clean glass flask, and 400 mL of a 0.1 M zinc oxide solution was added gradually under continuous stirring to initiate the reaction. The observable colour variation, besides the formation of a whitish precipitate, indicated the successful synthesis of ZnO nanoparticles. The reaction was allowed to proceed until bubble formation stopped, confirming completion. The resulting precipitate was then washed repeatedly with distilled water and methanol towards remove any remaining contaminants or unreacted components. To finish, the purified nanoparticles were dried in a hot-air oven at 60°C to obtain powdered ZnO nanoparticles (El-Khawaga *et al.* 2025; Mahajan *et al.* 2025; Abdulqodus *et al.* 2025; Al Hinai *et al.* 2026).

2.3 Analytical Methods

These developments, in addition to analytical work from this green fabrication of ZnO nanoparticles stayed analyzed using several advanced characterization techniques. The UV–Vis concentration range of the reaction mixture be located detailed by at UV-1800 model by Shimadzu, working within the 200 to 800 nm spectral range, and the appearance of a representative absorption peak established the successful development of ZnO nanostructures. The stability and surface charge of the nanoparticles were evaluated using zeta potential analysis. The particle size and size distribution were determined through photon correlation spectroscopy (PCS) using a Zetasizer 3000 (Malvern Instruments, UK). The measurements were conducted at 25°C and a 90° scattering angle, providing the z-average particle size and the PDI, which indicate the uniformity of the nanoparticle dispersion. FTIR was performed using an Alpha Bruker spectrometer (Pike Technologies) to recognize the well-designed clusters that *Moringa Oleifera* leaf mine contributed to reducing, stabilizing, and capping the ZnO nanostructures. This ranges stayed verified trendy ATR method over a variety of 4000–400 cm^{-1} by a determination from 4 cm^{1}. The surface texture of these ZnO nanoparticles was observed using a Carl Zeiss-EVS 180 SEM. A small amount of the nanoparticle suspension remained after loading onto a carbon-coated copper grid, any extra fluid was taken up by staining, and this trial be situated air-dried before imaging. The elemental composition was determined using EDX attached to the SSX-550 SEM-EDX system. XRD analysis was carried out to study the crystal particle assembly and estimate the crystal particle size of the ZnO NPs. About 100µL from this dried model was placed and analyzed using an X-ray diffractometer (Model 1130/90 JDPS) operating at 30 keV and 40 mA through Cu Kα radiation. This diffusion configuration was used to complete a 2θ range of 10°–80°, sanctioning the transparent nature about this produced nanostructures (Ali *et al.* 2025; Vidaarth *et al.* 2024; Kumawat *et al.* 2025; Elabbasy *et al.* 2025).

2.4 Photocatalytic Removal of Dyes by Biosynthesized ZnO NPs

This photocatalytic presentation about the green-synthesized ZnO NPs was evaluated using two synthetic dyes, Methylene Orange (MO) and Malachite Green (MG). All degradation experiments were carried out under direct sunlight. To prepare the stock dye solutions, 10mg of each dye was precisely weighed and dissolved in 100 mL of distilled water. From these stock solutions, dye concentrations of 100, 200, and 300 mg/l were obtained through serial dilution. For each photocatalytic trial, 30mg of ZnO nanoparticles was introduced into 100ml of the dye solution and mixed thoroughly. Before exposing the mixture to sunlight, the solution was stirred using a magnetic stirrer for about 30 min to achieve binding–release stability between dye particles and the surface of this substance. At regular time intervals, 5ml from this reaction mixture was reserved, then its absorbance was measured using a UV–Vis apparatus to track the extent of dye degradation. A noticeable colour transition from a strongly coloured solution to a nearly colourless one was observed within 60 minutes, indicating significant photocatalytic activity (El-Khawaga *et al.* 2025; Younas *et al*. 2025; Purushotham *et al.* 2025; Yadav *et al.* 2025). This deprivation competence can be situated designed by the following principle is

$$\text{Percentage of dye deprivation} = C_0 - C_t / C_0 \times 100$$

2.5 Degradation Kinetics Study

The kinetic behaviour of the photocatalytic degradation process was investigated through pseudo-zero, pseudo-first, and pseudo-second-order kinetic frameworks (Sahu *et al.* 2025). These models help in understanding the degradation mechanism and the rate-controlling steps involved. This photocatalytic degradation of dyes was initially examined by the pseudo-first prototypical, conveyed for instance of $C_t = C_0 \ e^{-Kt}$ ----------- (1). This pseudo-second prototypical was likewise applied to analyze the adsorption-driven degradation mechanism. The linearized system from the pseudo-second prototypical equality from this $t / qt = (1/ qe)t + 1 / k_2qe^2$-------(2). The degradation kinetics of all dye concentrations were also examined using the L–H prototypical, which is extensively used to describe heterogeneous photocatalytic reactions. This L–H model effectively relates the reaction rate to both adsorption and degradation processes occurring on the catalyst surface (Ramaprabha *et al.* 2025; Sharafzadeh *et al.* 2025).

3. RESULT AND DISCUSSION

3.1 Optical Properties from ZnO NPs

This formation of ZnO NPs was primarily indicated by the appearance of a white precipitate when the *Moringa Oleifera* foliage mine was mixed with the zinc precursor solution. This colour change signified the successful reduction of zinc ions and the formation of ZnO. This visual behaviour of the synthesized ZnO NPs was examined by UV–Vis spectroscopy. A noticeable absorption peak was observed at 369nm, which corresponds to the representative SPR of ZnO NPs. This peak confirms these occurrences from abundant surface electrons and further verifies the successful synthesis of ZnO NPs. These UV–Vis spectra scale from the green fabrication of ZnO NPs presented in Figure 2, and the results align well with earlier reported studies.

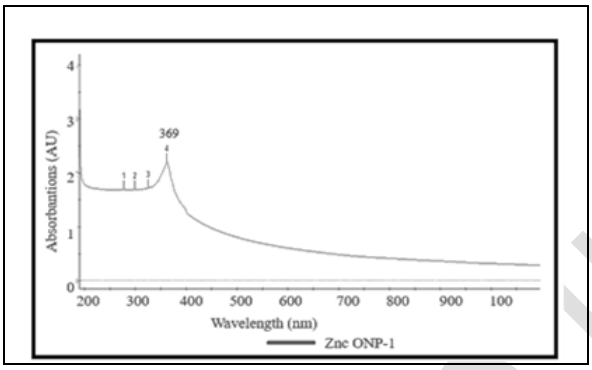

Fig. 2: UV–is optical spectrum of eco-synthesized ZnO NPs using *Moringa Oleifera* foliage mine

3.2 FT-IR Analysis from ZnO NPs

The chemical groups involved in the eco-friendly synthesis and stability of ZnO NPs were investigated by FT-IR spectroscopy. The spectrum is shown in Figure 3. The broad band at 3436 cm^{-1} indicates O-H bond vibration. This confirms their presence from hydroxyl/phenol compounds from *Moringa Oleifera* leaves' mine. The band at 2927 cm^{-1} is attributed to C-H bond vibration from alkanes. The bands at 1638 cm^{-1} and 1413 cm^{-1} are attributed to C=C bond vibrations from aromatic compounds. This confirms the presence of flavonoids and polyphenolic compounds from *Moringa Oleifera* leaf extract. The bands at 1030 cm^{-1} and 866 cm^{-1} are attributed to C-O and C-N bond vibrations from compounds. The characteristic band at 543 cm^{-1} is attributed to Zn-O bond vibrations. This confirms their presence in ZnO NPs. These results from FT-IR spectroscopy confirm that phytochemicals present during synthesis from *Moringa Oleifera* leaves' extract play a significant role in reducing zinc ions and preventing their aggregation in biosynthesizing ZnO NPs.

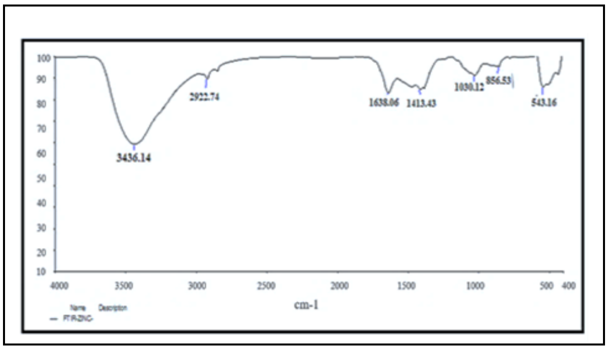

Fig. 3: FT-IR apparatus from green fabrication ZnO NPs using *Moringa Oleifera* leaf extract

3.3 Particle Size Analysis of ZnO NPs

The particle size distribution of these green-fabricated ZnO NPs was evaluated using DLS; the corresponding report is shown in Figure 4. The analysis revealed a Z-average particle size of 102.4nm, indicating that the nanoparticles formed were predominantly in the nanoscale range. The PDI remained at 0.143, which reflects a narrow size distribution and confirms the uniformity of the synthesized nanoparticles. A major intensity peak was observed at 131.7nm, suggesting that most particles were clustered around this size range. The DLS data also showed D10, D50, and D90 values of 69.1nm, 117nm, and 201nm, respectively, further supporting that the majority of the particle population lies within a controlled and predictable size range. The overall quality of this consequence remained marked as "Good," sanctioning the dependability of this quantity. The outcomes indicate that these phytochemicals existing in Moringa Oleifera effectively facilitated the establishment of stable, well-dispersed ZnO nanoparticles with a narrow size distribution. The controlled particle size observed in this study enhances the photocatalytic efficiency of the ZnO NPs and supports their suitability for dye degradation applications.

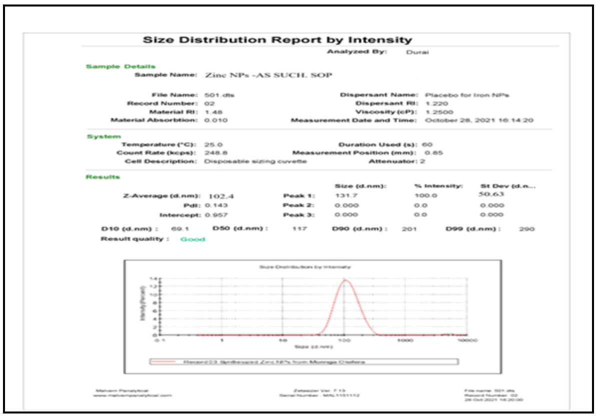

Fig. 4: Particle size distribution from green-fabricated ZnO NPs obtained from *Moringa Oleifera* leaf extract

3.4 SEM Analysis of ZnO NPs

The above SEM analysis of ZnO NPs synthesized by the present *Moringa Oleifera* leaf mine confirms the presence of the above morphological characteristics of ZnO NPs, as shown in Figure 5. The micrograph shows the presence of agglomerated clusters of ZnO nanoparticles, which is a general trend in green-synthesized metal oxide nanoparticles due to the presence of the above agents. The ZnO NPs have irregular and granular shapes with nanometric dimensions, which confirms the formation of ZnO nanoparticles. The surface texture of the ZnO NPs appears to be rough and compact, which confirms the presence of high intermolecular interaction due to the presence of phytochemicals. The above observations confirm the green synthesis of ZnO NPs with a uniform surface structure.

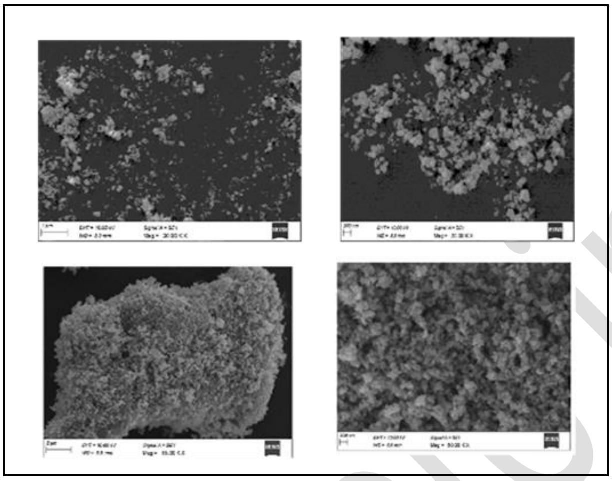

Fig. 5: SEM images of green-synthesized ZnO NPs by *Moringa Oleifera* foliage mine

3.5 EDX Investigation from Zno Nps

These primary structures developed in ZnO NPs were analyzed using EDX spectroscopy, and in addition, the spectrum for ZnO NPs is represented in Figure 6. In this EDX spectrum, two high peaks for Zn and O elements confirm the successful development of ZnO NPs. The high peak for Zn indicates that zinc is present in high percentages in ZnO NPs. In addition, the peak for O confirms that ZnO NPs are oxide in nature. Quantitatively, it has been identified that zinc is present at 84.09% and O at 15.91%. This indicates that ZnO NPs are in accordance with the stoichiometric composition. In addition, the absence of peaks for other elements in the EDX spectrum confirms that synthesized ZnO NPs are devoid of impurities. This indicates that *Moringa Oleifera* leaf extract has acted effectively, for instance, in dropping and stabilizing representative elements in this green method for synthesizing ZnO NPs.

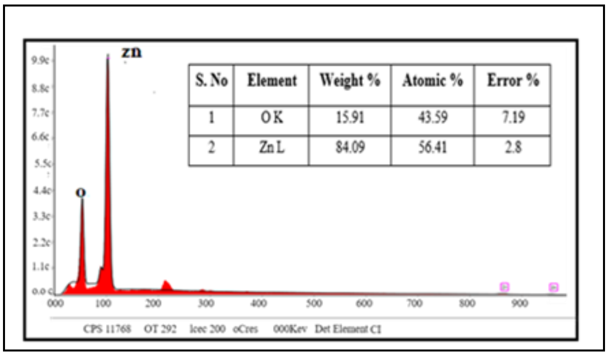

S. No	Element	Weight %	Atomic %	Error %
1	O K	15.91	43.59	7.19
2	Zn L	84.09	56.41	2.8

Fig. 6: EDX investigation from ZnO nanoparticles synthesized from *Moringa Oleifera* leaf extract

3.6. XRD Analysis of Zno Nps

The crystallized structures from these biosynthesized ZnO NPs be present in investigations by XRD, besides the corresponding diffraction pattern is shown in Figure.7. In the diffractogram, sharp and intense peaks are observed by 2θ values ranging from 31.8°, 34.4°, 36.3°, 47.5°, 56.6°, 62.8°, 66.3°, 67.9°, 69.1°, 72.5°, as well as 76.9°. These sharp and intense peaks are indexed to the (100), (002), (101), (102), (110), (103), (200), (112), (201), (004), and (202) crystal peaks, which are representative of the hexagonal quartzite structures of ZnO. All these peaks are indicative of a match with the typical JCPDS 36-1451, indicating that these synthesized nanoparticles have a pure hexagonal phase without any impurities and subordinate segments. These sharp and intense peaks are indicative of high crystallinity, showing that the biosynthesis route by *Moringa Oleifera* foliage mine, for instance, emerald dipping, besides alleviating mediator, is effective. Moreover, these calculated crystallite sizes are in the nanometer region, supporting these positive findings about ZnO NPs through this eco-friendly synthesis route.

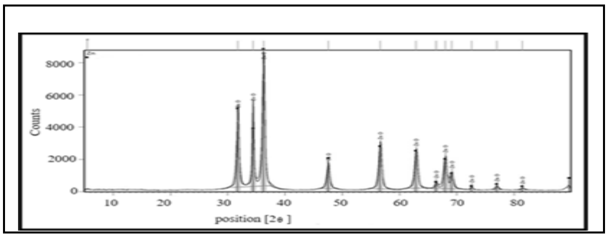

Fig. 7: XRD investigation of ZnO NPs fabricated from *Moringa Oleifera* leaf extract

3.7 Photocatalytic Degradation of Dyes Investigation from ZnO NPs

3.7.1 Methylene Orange Dye (MO)

The photocatalytic efficiency of these biosynthesized ZnO NPs was continued to be monitored in terms of the degradation of MO dye under visible light irradiation, and all these results are represented in Figure 8 (a–c). In this degradation study, continuous reduction in the color intensity of the MO dye solution was visually monitored with the passage of time, which indicates continuous degradation of MO dye molecules in the presence of ZnO NPs. The UV–vis absorption spectra in Figure 8 (b) further confirm this trend, in which this specific absorption peak for MO dye in the region around 460 nm continuously decreased with the increase in irradiation time (0–180 min). This continuous reduction in absorption spectra indicates efficient photocatalytic activity for synthesized ZnO NPs. In Figure 8 (c), the percentage degradation for different concentrations of ZnO NPs is represented, in which maximum efficiency was observed for a 30 mg catalyst dosage, with 76% degradation efficiency after 180 minutes. This indicates that a higher catalyst dosage would provide more active sites for efficient degradation of dye molecules. In order to confirm the degradation mechanism for MO dye in the presence of ZnO NPs, different kinetic models like zero-order, first-order, and second-order models were supported by using linear plots for all three models, which are represented in Figure 9 (a–c). In all three models, first-order kinetics showed maximum linear behavior ($R^2 \approx 0.998$). This indicates that this deprivation in MO dye monitors first-order kinetics. This indicates that the rate of dye degradation would be mainly influenced by the initial concentration of MO dye present in the solution.

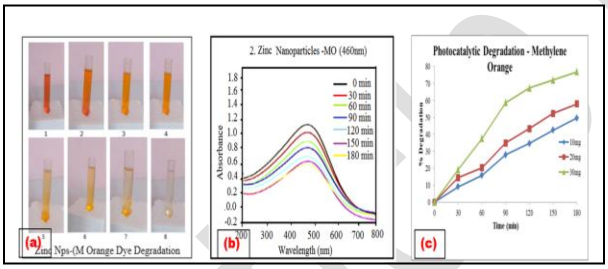

Fig. 8: (a) Effect of ZnO NPs on MO dye, (b) UV−visible absorption spectra, and (c) Photocatalytic degradation of the dye

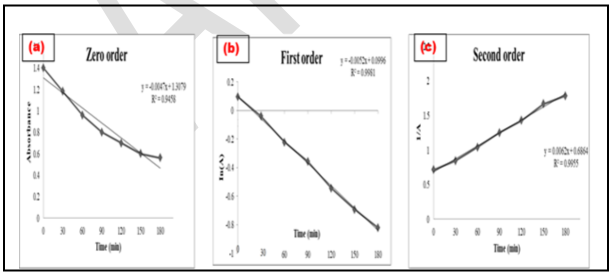

Fig. 9: Kinetic profile of MO dye degradation showing (a) zero-order, (b) first-order and (c) second-order reactions

3.7.2 Malachite Green Dye (MG)

The photocatalytic activity of these biosynthesized ZnO NPs was evaluated by monitoring the degradation of MG dye under visible light irradiation, and the results are presented in Figure 10 (a-c). A gradual change in the color of the dye solution was observed during this reaction, which confirms the degradation of MG dye. The UV-Vis absorption ranges in Figure 10 (b) show a constant decrease in the distinct absorption peak of MG dye at 624 nm with an increase in irradiation time from 0 to 180 minutes. This constant decrease in absorbance intensity shows the degradation of dye molecules by the ZnO nanoparticles. The photocatalytic degradation efficiency of the dye by these various dosages of ZnO NPs is presented in Figure 10 (c). Among these tested concentrations of ZnO NPs (10 mg, 20 mg, and 30 mg), the highest degradation efficiency of nearly 91% was observed at 30 mg of ZnO NPs, which confirms that higher dosages of ZnO NPs exhibit higher photocatalytic efficiency. To understand this reaction mechanism, these kinetic studies were carried out using zero-, first-, and second-order kinetic models, which were presented in Figure 11 (a-c). Among these first-order models, the highest linear relationship was observed, which confirms that the photodegradation of MG dye takes place following first-order kinetics, where the response percentage is primarily determined by the dye concentration. This zero-order model shows a moderate relationship, while this second-order model shows the least relationship with the experimental data. These biosynthesized ZnO nanoparticles from these leaf extracts exhibit photocatalytic efficiency, which results in rapid decolorization of MG dye. These results confirm that these green-fabricated ZnO NPs are promising, biodegradable, and economical photocatalysts for the treatment of dye-contaminated wastewater.

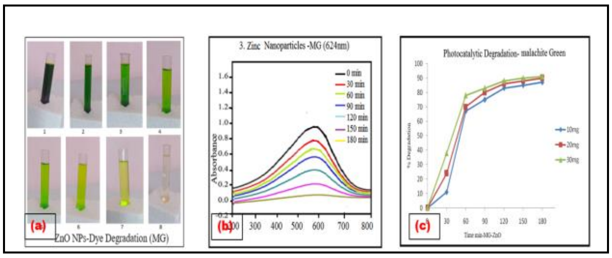

Fig. 10: (a) Influence of ZnO NPs on MG dye, (b) UV–vis absorption ranges and (c) Photocatalytic degradation of the dye

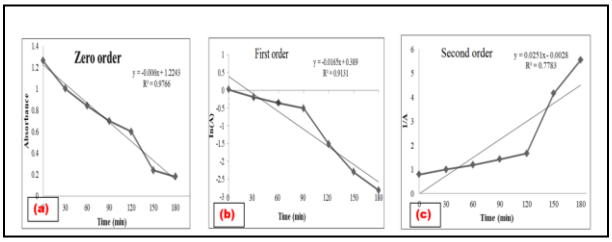

Fig. 11: Kinetic modelling of MG dye degradation showing (a) zero-order, (b) first-order and (c) second-order reactions

4. CONCLUSION

In this research work, ZnO NPs can be effectively fabricated using *Moringa Oleifera* leaf extract, proving that plant-based compounds can serve as an effective and eco-friendly alternative to chemical reducing agents.

The sharp diffraction peaks showed that the particles are highly crystalline and fall within the nanoscale range.

The optical analysis, supported by UV–Visible spectroscopy, verified the formation of ZnO NPs and showed absorption features suitable for photocatalytic applications.

The green-synthesized ZnO nanoparticles exhibited excellent photocatalytic performance, achieving 76% degradation of Methyl Orange and 91% degradation of Malachite Green under visible light. These findings demonstrate their potential as an eco-friendly photocatalyst for wastewater treatment. Future research should focus on optimizing the synthesis process, evaluating performance in real wastewater, and assessing long-term stability for large-scale applications.

The photocatalytic degradation of both dyes followed first-order kinetics, confirming the high efficiency of the green-synthesized ZnO nanoparticles. Their excellent performance is attributed to their small particle size, high surface area, and good crystallinity, highlighting their potential for sustainable wastewater treatment and environmental remediation.

Moringa Oleifera is increasingly preferred by researchers because it is abundant, inexpensive, environmentally friendly, and rich in bioactive phytochemicals that act as natural reducing and stabilizing agents in green nanoparticle synthesis. Its use minimizes hazardous chemicals while producing stable nanoparticles with enhanced functional properties.

Future research should focus on large-scale synthesis, optimization of process parameters, detailed toxicity and biocompatibility studies, catalyst reusability, and the application of *Moringa Oleifera*-mediated nanoparticles in environmental remediation, biomedical fields, and industrial wastewater treatment.

FUNDING

There are no financial conflicts of interest to disclose. No funding is provided for carrying out the research work.

CONFLICT OF INTEREST

The authors have no conflicts of interest to declare.

COPYRIGHT

REFERENCES

Abdelhameed, R. E., Galilah, D. A. and Metwally, R. A., Multifaceted role of *Moringa Oleifera* leaf extract as antimicrobial, growth enhancer and mitigator of salt stress in tomato seedlings, *BMC Plant Bio.*, 25(1), 1144(2025). https://doi.org/10.1186/s12870-025-07149-7

Abdulqodus, A. N., Abdulrahman, A. F., Mostafa, S. H., Kareem, A. A., Hamad, S. M., Ahmed, S. M., Munirah, A. A. and Dilshad, S., Green synthesis of ZnO nanoparticles: effect of pH on morphology and photocatalytic degradation efficiency, *Appl. Phys. A.*, 131(9), 720(2025). https://doi.org/10.1007/s00339-025-08874-4

Aghajanyan, A., Timotina, M., Manutsyan, T., Ani, H., Mikayel, G., Robin, S., Sofia, A., Karen, T., Lilit, G. and Liana, G., A novel approach for synthesizing silver nanoparticles with antibacterial and cytotoxic activities using the leaf extract of hydroponically grown *Moringa Oleifera*, *Sci. Rep.*, 15(1), 16637(2025). https://doi.org/10.1038/s41598-025-01023-0

Al Hinai S, Al Hinai A, Almansouri HE, Al Haddabi Q, Al Maqbali H, Al Rubaii AY. Impact of drying techniques on the structural properties and methyl orange degradation efficiency of Moringa oleifera mediated ZnO nanoparticles, Next Materials. 1(12),102102(2026). https://doi.org/10.1016/j.nxmate.2026.102102

Ali, A. B. M., Mohammed, A. A., Singh, N. S. S., Ali, R. M., Akmal, A., Bakhodir, S., Lola, S., Aseel, S., Ali, A. I., Islam, S. and Khan, M. I., Green synthesized Zinc oxide nanoparticles mediated by Thymus pannonicus extract as a novel catalyst in the reduction of aromatic nitro compounds, *J. Organomet. Chem.*, 1040, 123817(2025). https://doi.org/https://doi.org/10.1016/j.jorganchem.2025.123817

de Souza, L. R., de Azevedo, E. C., Dutra, J. M., Carlos, D. S. W., Nunes, C. E. E., Damiani, C. and Boas, B. V. E. V., Natural plant pigments: genes and transcription factors regulating synthesis and degradation, extraction, microencapsulation, food applications, and sensory impacts, *Food Sci.*

Biotechnol., 35(4), 731-761(2026). https://doi.org/10.1007/s10068-025-01982-0

Elabbasy, M. T., Bayomi, R. M. E., Abdelkarim, E. A., Abd, E. E. H., Othman, M. S., Mohamed, E. G., Mai, A. S., Muteb, H. A., Fahad, A. A., Tamer, E. and Mohamed, A. H., Antibacterial and Antibiofilm Activity of Green-Synthesized Zinc Oxide Nanoparticles Against Multidrug-Resistant Escherichia coli Isolated from Retail Fish, *Mol.*, 30(4), 768(2025). https://doi.org/10.3390/molecules30040768

El-Khawaga, A. M., Elsayed, M. A., Gobara, M., Ahmad, A., Amr, H. H., Zaher, A. A., Mohsen, M. and Salem, S. S., Green synthesized ZnO nanoparticles by Saccharomyces cerevisiae and their antibacterial activity and photocatalytic degradation, *Biomass Convers. Biorefine*., 15(2), 2673–2684(2025). https://doi.org/10.1007/s13399-023-04827-0

El-Sheekh, M. M., El-Kassas, H. Y. and Ali, S. S., Microalgae-based bioremediation of refractory pollutants: an approach towards environmental sustainability, *Microb. Cell Fact*., 24(1), 19(2025). https://doi.org/10.1186/s12934-024-02638-0

Farrag, A. M., Awad, M. E., Aboelnga, M. M. and El-Bindary, A. A., Enhancement of commercial dye photocatalytic degradation through the use of silver-doped kaolinite-zinc oxide quantum dots, *BMC Chem.*, 19(1), 291(2025). https://doi.org/10.1186/s13065-025-01648-2

Gul, S., Nazar, M., Sharif, M. N., Rida, T., Fatima, I., Ayesha, S., Anas, M. Z., Rubab, S. and Mustafa, Z., Advanced Nanotechnology in Wastewater Treatment: Investigating the Role of Nanoparticles in Pollutant Removal, Water Recovery, and Environmental Sustainability, *Scholars J. Eng. Technol.*, 13(5), 331–356(2025). https://doi.org/10.36347/sjet.2025.v13i05.004

Kristanti, R. A., Hadibarata, T., Niculescu, A., Dan, E. M. and Mihai, A. G., Nanomaterials for Persistent Organic Pollutants Decontamination in Water: Mechanisms, Challenges, and Future Perspectives, 15(14), 1133(2025). https://doi.org/10.3390/nano15141133

Kumar, M., Singh, V. P., Bhat, S. B. and Kumar, R., Environmental risks of textile dyes and photocatalytic materials for sustainable treatment: current status and future directions, *Discov. Environ.*, 3(1), 132(2025). https://doi.org/10.1007/s44274-025-00337-0

Kumawat, G., Rajpurohit, D., Vyas, D., Ali, B. A., Kumar, S. U. and Jain, D., Characterization of green-synthesized zinc oxide nanoparticles and its influence on post-harvest shelf-life of garlic against black mold disease caused by Aspergillus niger, *Front Microbio.*, 16, 1532593(2025). https://doi.org/10.3389/fmicb.2025.1532593

Lee, J., Woo, S., Park, T. and Hong, S., Development of nanofiltration-based irrigation and wastewater reuse technologies for sustainable water resource security, *Desalin.*, 638, 120507(2026). https://doi.org/10.1016/j.desal.2026.120507

Mahajan, M., Kumar, S., Gaur, J., Sandeep, K., Dalal, J., Singh, G., Misra, M. and Singh, A. D., Green synthesis of ZnO nanoparticles using Justicia adhatoda for photocatalytic degradation of malachite green and reduction of 4-nitrophenol, *RSC Adv*., 15(4), 2958–2980(2025). https://doi.org/10.1039/d4ra08632e

Vidaarth, T.N., Surendhiran, S., Jagan, K.S.G., Savitha, S., Balu, K.S., Karthik, A. and Kalpana, B., 2024. Surface chemistry of phytochemical enriched MgO nanoparticles for antibacterial, antioxidant, and textile dye degradation applications. *Journal of Photochemistry and Photobiology A: Chemistry*, *448*, p.115349. https://doi.org/10.1016/j.jphotochem.2023.115349

Muthusamy, K., Duraisamy, V., Giri, J., Prem, G., Husain, A., Vicki, V. W. and Kanan, M., Green synthesis of silver/zinc oxide plasmonic nanocomposites using *Moringa Oleifera*: A dual-function strategy for photocatalysis and dye-sensitized solar cell performance, *J. Sci. Adv. Mater. Dev.*, 10(3), 100954(2025). https://doi.org/https://doi.org/10.1016/j.jsamd.2025.100954

Nair, S., Mol, J. J. S., Samuel, G. and Kothakota, A., Improved mechanical characteristics and shelf life of sustainable biodegradable food packaging films via integration of rice straw nanocellulose, *Moringa Oleifera* extract and gelatin, *Int. J. Bio. Macromol*., 321, 145977(2025). https://doi.org/https://doi.org/10.1016/j.ijbiomac.2025.145977

Nguyen, N. T. T., Phan, A. N. Q., Tran, T. V. and Nguyen, T. T. T., Morinda citrifolia fruit extract-mediated synthesis of ZnO and Ag/ZnO nanoparticles for photocatalytic degradation of tetracycline, *Environ. Res.*, 273, 121209(2025). https://doi.org/https://doi.org/10.1016/j.envres.2025.121209

Olajide, O. O., Emmanuel, S. A. and Fayomi, O. M., Green Synthesis, Characterization, and In Vivo Anti-Plasmodial Activity of Copper Oxide Nanoparticles Using *Moringa Oleifera* Leaf Extract, 4(1), 31–39(2025). https://doi.org/10.34172/jbp.2025.5.

Periyasamy, A. P., Textile Dyes in Wastewater and its Impact on Human and Environment: Focus on Bioremediation, *Water, Air, Soil Pollut.*, 236(9), 562(2025). https://doi.org/10.1007/s11270-025-08204-7

Purushotham, D., Ramesh, A. M., Thimmappa, D. S. and Kalegowda, N., Green Synthesis of Zinc Oxide Nanoparticles Using Aqueous Extract of Pavonia zeylanica to Mediate Photocatalytic Degradation of Methylene Blue: Studies on Reaction Kinetics, Reusability and Mineralization, *Int. J. Mol. Sci.*, 126(10), 4739(2025). https://doi.org/10.3390/ijms26104739

Ramaprabha, K. and Kumar, S. V., Effective photocatalytic degradation and kinetic modelling of azo dyes by zinc oxide nanoparticles from Brevibacterium casei, *Desalin. Water Treat.*, 321, 100936(2025). https://doi.org/https://doi.org/10.1016/j.dwt.2024.100936

Rotimi, L., Oyebamiji, A. K., Ajayi, A., Agoro, M. A. and Meyer, E. L., Synthesis of Silver Nanoparticles with Aqueous Extract of *Moringa Oleifera* Lam Leaves and Its Ameliorative Effect on Benign Prostatic Hyperplasia (BPH) in Wistar Rat: Experimental and Computational Approaches, *J. Phytomed. Ther.*, 24(1), 2210 – 2230. https://doi.org/10.4314/jopat.v24i1.34

Sahu, R. K. and Gangil, S., Insights into biopolymeric transitions during thermal degradation and kinetic parameters for Chickpea stalk (Cicer arietinum), *Process Saf. Environ. Prot.*, 195, 106766(2025). https://doi.org/https://doi.org/10.1016/j.psep.2025.01.020

Sarwar, K., Nazli, Z. H., Munir, H., Aslam, M. and Ahlam, K., Biosynthesis of zinc oxide nanoparticles using *Moringa Oleifera* leaf extract, probing antibacterial and antioxidant activities, *Sci. Rep.*, 15(1), 20413(2025). https://doi.org/10.1038/s41598-025-08839-w

Sharafzadeh, S., Zolgharnein, J., Nezamzadeh–Ejhieh, A. and Farahani, S. D., A co-precipitation synthesized Zn(II)/Ni(II) magnetic heterostructure ferrite for photocatalytic degradation of metronidazole: Charge carriers transfer mechanism, kinetics and thermodynamic aspects, *Int. J. Hydrogen Energy*, 106, 1429–1442(2025). https://doi.org/https://doi.org/10.1016/j.ijhydene.2025.02.031

Shinde, A., Patwardhan, S., Kshirsagar, R., Jivani, F., Loni, S., Manju, T., Guldhe, A. and Penna, S., Agricultural Waste Biomass Management and Biochar Production, *Biochar: Precious Resource Bio. Waste*, 115–153(2025). https://doi.org/10.1007/978-981-95-0425-1_6

Singh, A., Gupta, A., Prasad, B., Ghai, K. and Sonu, D., A facile green synthesis of bismuth oxide nanoparticles (BiONPs) mediated through bark extract of *Moringa Oleifera* lam. And characterisation, *Discov. Chem.*, 2(1), 201(2025). https://doi.org/10.1007/s44371-025-00278-w

Tella, T. A., Festus, B., Olaoluwa, T. D. and Oladapo, A. S., Chapter 15 - Water and wastewater treatment in developed and developing countries: Present experience and future plans, *Smart Nanomater. Environ. Appli.*, 351–385(2025). https://doi.org/10.1016/B978-0-443-21794-4.00030-2

Thakur, A., Gupta, R., Thakur, S., Shivam, S., Sahil, T. T. and Devi, A., Development and Characterization of Copper Oxide and Copper-Zinc Oxide Nanoparticles Synthesized Using *Moringa Oleifera*: Photocatalytic and Antibacterial Applications, *J. Neonatal Surgery*, 14(13s), 388–397(2025). https://doi.org/10.52783/jns.v14.3253

Yadav, S., Singh, P., Varshney, G., Saurabh, Singh, P. and Kaur, R., Photocatalytic degradation of crystal violet dye using phytofabricated zinc oxide nanoparticles from anthocyanin extract, *Microchem. J.*, 213, 113681(2025). https://doi.org/https://doi.org/10.1016/j.microc.2025.113681

Younas, M. U., Iqbal, M., Ahmad, N., Iqbal, S., Abida, K., Arif, N., Osma, M. A. and Anjum, F., Biogenic synthesis of zinc oxide nanoparticles using NARC G1 garlic (Allium sativum) extract, their photocatalytic activity for dye degradation and antioxidant activity of the extract, *Res. Chem.*, 13, 102035(2025). https://doi.org/https://doi.org/10.1016/j.rechem.2025.102035

Zhao, D., Yuan, F., Ren, Y., Li, Y., Zhou, K., Huang, X., Fu, C. and Gong, Z., High-performance Ti3C2-mediated adsorptive membrane for selective lithium recovery from shale gas wastewater, *Desalin.*, 638, 120506(2026). https://doi.org/10.1016/j.desal.2026.120506